

# PRISM: Streaming Human Motion Generation with Per-Joint Latent Decomposition

Zeyu Ling<sup>1\*</sup>, Qing Shuai<sup>1\*</sup>, Teng Zhang<sup>3\*</sup>, Shiyang Li<sup>1</sup>, Bo Han<sup>3</sup>, and Changqing Zou<sup>1,2</sup>

<sup>1</sup> State Key Laboratory of CAD & CG, Zhejiang University, Hangzhou, China  
changqingzou@zju.edu.cn

<sup>2</sup> Zhejiang Lab, Hangzhou, China

<sup>3</sup> Computer Animation & Perception Group, Zhejiang University, Hangzhou, China

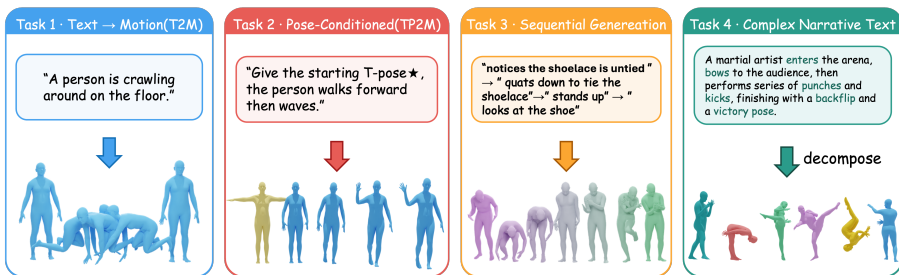


**Fig. 1:** A single PRISM model handles text-to-motion, pose-conditioned generation, sequential synthesis, and narrative motion composition, producing coherent streaming motion with 10+ segments far beyond the training horizon.

**Abstract.** Text-to-motion generation has advanced rapidly, yet two challenges persist. First, existing motion autoencoders compress each frame into a single monolithic latent vector, entangling trajectory and per-joint rotations in an unstructured representation that downstream generators struggle to model faithfully. Second, text-to-motion, pose-conditioned generation, and long-horizon sequential synthesis typically require separate models or task-specific mechanisms, with autoregressive approaches suffering from severe error accumulation over extended rollouts.

We present PRISM, addressing each challenge with a dedicated contribution. **(1)** A *joint-factorized motion latent space*: each body joint occupies its own token, forming a structured 2D grid (time × joints) compressed by a causal VAE with forward-kinematics supervision. This simple change to the latent space—without modifying the generator—substantially improves generation quality, revealing that latent space design has been an underestimated bottleneck. **(2)** *Noise-free condition injection*: each latent token carries its own timestep embedding, allowing conditioning frames to be injected as clean tokens (timestep 0) while the remaining tokens are denoised. This unifies text-to-motion and pose-conditioned generation in a single model, and directly enables autoregressive segment chaining for streaming synthesis. Self-forcing training further suppresses

<sup>0</sup> \*Equal contribution.

drift in long rollouts. With these two components, we train a single motion generation foundation model that seamlessly handles text-to-motion, pose-conditioned generation, autoregressive sequential generation, and narrative motion composition, achieving state-of-the-art on HumanML3D, MotionHub, BABEL, and a 50-scenario user study. Code will be open-sourced at <https://github.com/ZeyuLing/PRISM>.

**Keywords:** Human motion generation · Per-joint latent decomposition · Flow matching · Streaming generation

## 1 Introduction

Text-driven 3D human motion generation aims to synthesize realistic and physically plausible human movements from natural language descriptions. With the growing demand for high-quality motion content in games, films, virtual reality, and embodied AI, this task has attracted increasing research attention. Recent advances have been fueled by large paired datasets [7, 10, 17, 18] and powerful generative architectures, including diffusion models [4, 30, 40], flow matching approaches [5, 13], and autoregressive transformers [7, 9, 15, 38].

Despite this progress, generated motions still exhibit artifacts such as jitter, foot sliding, ground penetration, and unnatural transitions, especially in long or physically demanding sequences. Recent efforts have primarily focused on improving the generator itself—scaling model capacity [7, 16], adopting stronger training objectives [5, 13], or curating larger datasets [17, 18]. Comparatively little attention has been paid to the design of the *motion latent space*, which mediates between raw motion signals and the generative model.

We argue that this is a critical oversight. Existing motion autoencoders [4, 9, 35, 38] compress each frame into a single, high-dimensional latent token, concatenating global trajectory, per-joint rotations, and auxiliary signals into a monolithic code. The downstream generator must implicitly disentangle these heterogeneous signals—which have different physical units, scales, and temporal dynamics—before it can model them, consuming capacity that would otherwise go to semantic understanding. This limitation is visible across recent milestones: MLD [4] pioneered latent diffusion for motion but retains a single-token-per-frame bottleneck; ViMoGen [16] pushes quality through data and model scaling yet still uses a flattened latent; MotionStreamer [35] introduces streaming autoregressive diffusion but focuses on the generation paradigm rather than the latent design. None of these methods systematically rethinks the *granularity* of motion tokenization.

Our key observation is that human motion is inherently structured along the kinematic tree: each joint has a distinct physical role and its rotation is intrinsically low-dimensional (6D). Existing methods ignore this structure by concatenating all signals into one vector per frame, forcing the generator to implicitly discover and disentangle the joint structure. We propose a **joint-factorized motion latent space**: each body joint—root trajectory, global orientation, and every articulated rotation—occupies its own token, forming

a structured 2D latent grid (time  $\times$  joints). A causal spatio-temporal VAE compresses this grid with forward-kinematics supervision. Empirically, merely replacing a monolithic latent space with our joint-factorized one—without any change to the generator architecture—substantially improves generation quality, providing strong evidence that *latent space design is as important as generator architecture*.

A second, independent challenge is that text-to-motion (T2M), pose-conditioned generation (TP2M), and long-horizon sequential synthesis are often treated as separate tasks, each requiring dedicated mechanisms such as inpainting networks [28], specialized positional encodings [1], or causal masking [35]. Moreover, autoregressive methods that chain multiple segments suffer from severe error accumulation, causing trajectory drift, motion degradation, and collapse.

We observe that these tasks share a common structural pattern: a prefix of the motion sequence is known (empty for T2M, an initial pose for TP2M, or the tail of a previously generated segment for autoregressive chaining), while the remaining tokens must be synthesized. Building on this observation, we introduce *noise-free condition injection*: each latent token carries its own timestep embedding, so the model can distinguish between noise-free conditioning tokens (timestep 0) and noisy generation targets. This mechanism unifies T2M and TP2M without architectural changes, and directly enables autoregressive segment chaining for unlimited-length streaming synthesis. A self-forcing training strategy [14] further suppresses drift by simulating the actual autoregressive inference pipeline during training, enabling stable generation over long rollouts with 10+ consecutive segments far beyond the training horizon of  $\leq 360$  frames ( $\sim 12$ s).

Building on these two contributions, we introduce **PRISM** (**P**er-joint **R**epresentation for **I**nfinite **S**treaming **M**otion):

**(1) A joint-factorized causal Motion VAE.** Each SMPL motion frame is decomposed along the kinematic tree into per-joint tokens. A causal spatio-temporal VAE compresses them into a structured 2D latent grid, preserving the factorized structure end-to-end. Forward-kinematics supervision bridges rotation and coordinate spaces. The factorized latent alone—without changing the generator—substantially boosts generation quality, because the generator can model per-joint dynamics directly.

**(2) Noise-free condition injection for streaming generation.** A flow-matching DiT generates motion over the latent grid. Each token carries its own timestep embedding: conditioning frames are injected as clean tokens while the rest are denoised. This unifies text-to-motion and pose-conditioned generation, and enables autoregressive streaming in a single model. Self-forcing [14] suppresses drift over long rollouts.

**(3) A single motion generation foundation model.** With these two components, we train a single model that seamlessly handles text-to-motion, pose-conditioned generation, and—by autoregressive chaining—sequential generation and narrative motion composition (Fig. 1). Trained on  $\sim 200$ K curated motion-text pairs from MotionHub [18], PRISM achieves state-of-the-art on HumanML3D

and MotionHub (text-to-motion and pose-conditioned generation), BABEL (sequential generation), and a 50-scenario user study on narrative composition.

## 2 Related Work

*Text-to-motion generation.* Text-driven motion generation spans VAE-based [3, 24], diffusion-based [4, 30, 40, 41], and flow-matching [5, 13] paradigms. Autoregressive and masked methods [9, 15, 22, 38] frame generation as token prediction over VQ codes or LLM backbones. Recent scaling efforts [16, 33] demonstrate that larger data and billion-parameter DiT architectures substantially improve generalization.

*Motion latent representations.* Motion latent space design has received less attention than generator architectures. Discrete tokenizers [7, 9, 15, 38] enable autoregressive prediction but incur compounding quantization error [4, 5]. Continuous VAEs [4, 13] avoid this but compress each frame into a monolithic vector. MoGenTS [37] first showed that per-joint discrete quantization improves quality by preserving kinematic structure, but is limited to single-clip VQ generation. Our method extends this to a continuous causal VAE in native SMPL rotation space with FK supervision, and enables streaming via noise-free condition injection.

*Long-horizon and streaming motion generation.* Generating coherent motion over multiple text descriptions remains challenging. DoubleTake [28] performs two-pass inpainting with a pre-trained diffusion prior; FlowMDM [1] introduces blended positional encodings for seamless transitions; TEACH [24] conditions on action labels. Recent streaming approaches—AMD [12], MotionStreamer [35], and ScaMo [21]—aim for unlimited-length generation but require task-specific architectures or suffer error accumulation over long rollouts. Our noise-free condition injection provides a generic chaining mechanism without architectural modification, and self-forcing [14] suppresses drift, enabling stable generation far beyond the training horizon.

*Unified motion generation models.* Several works [15, 32, 34, 36, 42, 45] pursue a single model across modalities (text, music, speech). Our work differs: rather than unifying input modalities, we unify *generation regimes* (text-to-motion, pose-conditioned, sequential, and narrative composition) within a single flow-matching model via noise-free condition injection.

## 3 Method

Given a text prompt (or a sequence of prompts for streaming generation), our goal is to generate high-quality, deployment-ready SMPL motion. PRISM consists of two tightly coupled components (Fig. 2): (1) a **joint-factorized causal Motion VAE** (Sec 3.1) that encodes SMPL motion into a structured 2D latent grid where each spatial position corresponds to a specific body joint, and (2) a **latent**

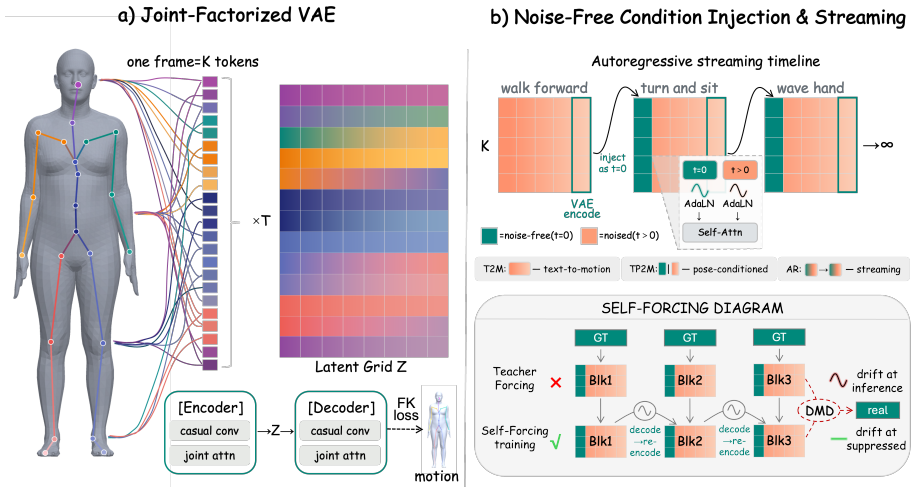


**Fig. 2: Overview of PRISM.** (a) A causal joint-factorized VAE compresses per-joint SMPL tokens into a structured 2D latent grid. (b) A flow-matching DiT denoises the grid with per-token timestep embeddings, unifying T2M, pose-conditioned generation, and autoregressive streaming via noise-free condition injection. Self-forcing suppresses drift over long rollouts.

**flow-matching DiT** (Sec 3.2) that generates motion by denoising this grid, using *noise-free condition injection* to unify text-to-motion, pose-conditioned generation, and autoregressive streaming within a single architecture.

### 3.1 Causal Joint-Factorized VAE

Existing motion autoencoders [4, 9, 35, 38] compress each frame into a single high-dimensional latent vector, concatenating root trajectory, per-joint rotations, and auxiliary signals into a monolithic code. This design creates three intertwined problems for large-scale motion generation. (i) **Latent entanglement**: the downstream generator must implicitly disentangle heterogeneous signals—which have different physical units, scales, and temporal dynamics—before it can model them, consuming capacity that would otherwise go to semantic understanding. (ii) **Non-causal encoding**: standard bidirectional convolutions require re-encoding the entire sequence to extend it by one frame, preventing incremental autoregressive generation. (iii) **Representation gap**: most methods operate in learned feature spaces (e.g., HumanML3D joint positions) rather than native body-model parameters, requiring post-hoc inverse kinematics for deployment.

We address all three problems with a single module: a *causal, joint-factorized* VAE that structures the latent space along the kinematic tree, encodes incrementally in time, and operates in native SMPL rotation space with forward-kinematics supervision.

*Joint-factorized input.* Given a motion sequence of  $T$  frames, the SMPL [20] body model parameterizes each frame by a root translation  $\mathbf{p}_i \in \mathbb{R}^3$ , a global orientation  $\boldsymbol{\theta}_i^0 \in \mathbb{R}^6$  (6D rotation [44] of the pelvis), and  $J$  joint rotations  $\{\boldsymbol{\theta}_i^j \in \mathbb{R}^6\}_{j=1}^J$ . Prior motion autoencoders [4, 9, 38] concatenate all of these into a single vector per frame. Instead, we organize each frame as  $K=J+2$  separate tokens, forming a 2D grid:

$$X = \left[ \underbrace{[\mathbf{p}_i; \Delta\mathbf{p}_i]}_{\text{root}}, \underbrace{\boldsymbol{\theta}_i^0}_{\text{orient.}}, \underbrace{\boldsymbol{\theta}_i^1, \dots, \boldsymbol{\theta}_i^J}_{\text{joint rotations}} \right]_{i=1}^T \in \mathbb{R}^{T \times K \times 6}, \quad (1)$$

where  $\Delta\mathbf{p}_i = \mathbf{p}_i - \mathbf{p}_{i-1}$  is the frame-to-frame displacement. Each token carries exactly one type of physical quantity with a uniform dimensionality of 6. As we show in Sec 3.2, this structured 2D grid is key to enabling per-token noise scheduling and noise-free condition injection.

*Encoder–decoder architecture.* The encoder maps  $X$  through residual blocks that alternate between two operations: *strictly causal temporal convolutions* that process each joint’s time series independently, and *spatial joint-attention layers* that let the  $K$  tokens within the same frame interact via multi-head self-attention, capturing kinematic couplings across joints (e.g., coordinated arm-leg swing, the rotation chain from hip to ankle). The output is a latent tensor  $Z \in \mathbb{R}^{T' \times K \times D}$  with  $T' = \lceil T/4 \rceil$  and  $D=16$ . The decoder mirrors this architecture. Spatial position  $k$  in the latent grid always corresponds to the same body joint, making the latent space semantically interpretable and, as we show in Sec 3.2, enabling per-token noise scheduling. All temporal convolutions are strictly causal—the receptive field at frame  $i$  covers only frames  $\leq i$ —so the VAE can encode new segments incrementally without reprocessing the entire history. A sliding-window feature cache [31] further ensures that both very short and arbitrarily long sequences can be handled with bounded memory. As shown in Tab. 5, the causal constraint incurs no loss in single-clip quality while enabling seamless multi-segment chaining that non-causal variants cannot perform.

*xz-plane data augmentation.* Standard motion capture datasets normalize each clip so that the first frame is centered at the origin and facing the positive  $z$ -axis. This convention holds for the first segment during autoregressive generation, but subsequent segments start from arbitrary positions and orientations in the  $xz$ -plane. To prevent the model from overfitting to the canonical starting pose, we apply random  $xz$ -plane translations and random rotations about the  $y$ -axis to each training clip. Without this augmentation, we observe noticeable jumps and trajectory drift at segment boundaries during autoregressive chaining.

*Forward-kinematics (FK) supervision.* The VAE is trained with:

$$\mathcal{L}_{\text{VAE}} = \lambda_{\text{param}} \mathcal{L}_{\text{param}} + \lambda_{\text{joints}} \mathcal{L}_{\text{joints}} + \lambda_{\text{traj}} \mathcal{L}_{\text{traj}} + \lambda_{\text{KL}} \mathcal{L}_{\text{KL}}, \quad (2)$$

where  $\lambda_*$  are scalar weighting coefficients,  $\mathcal{L}_{\text{param}}$  is an L1 loss on rotations and root trajectory, and  $\mathcal{L}_{\text{KL}}$  regularizes the posterior. Generating in rotation space

is desirable for deployment (output is directly compatible with SMPL [20] and animation rigs), but it creates a supervision gap: a small rotation error at a proximal joint (e.g.,  $1^\circ$  at the shoulder) cascades through the kinematic chain into a large positional error at distal joints (several cm at the wrist). Standard rotation-space losses treat all joints equally and miss this cascading effect. We address this with two FK-derived terms.  $\mathcal{L}_{\text{joints}}$  applies the deterministic FK mapping to the reconstructed rotations, computes *root-relative* 3D joint positions, and penalizes deviations from ground truth—directly catching cumulative rotation errors through their observable geometric effect.  $\mathcal{L}_{\text{traj}}$  supervises the *rollout trajectory* obtained by cumulative summation of the predicted frame-to-frame displacements  $\Delta\hat{\mathbf{p}}_i$ : we find that supervising the cumulative trajectory rather than per-frame displacements alone leads to faster convergence and significantly reduced jitter, because the cumsum formulation forces the model to account for how per-frame errors accumulate over time. In our tokenizer comparison (Sec 4.5), the joint-factorized latent alone—without any generator change—yields an  $18\times$  MPJPE improvement and  $20\times$  rFID reduction over monolithic baselines.

### 3.2 Latent Flow-Matching DiT with Noise-Free Condition Injection

Given the joint-factorized latent grid  $Z$ , we train a DiT-style [23] Transformer to generate motion via flow matching [19]. We adopt the architecture design of Wan [31] and ViMoGen [16], which has proven effective for latent generation tasks. Text conditioning is injected via cross-attention from latent tokens to embeddings produced by a frozen T5-XXL [27] encoder. Positional information is encoded through 2D rotary position embeddings (RoPE) [29] computed along both the temporal axis and the joint-index axis, enabling the Transformer to generalize to variable sequence lengths while exploiting the spatial structure of the joint-factorized grid.

*Flow-matching training.* We normalize the VAE latents to zero mean and unit variance using precomputed statistics, then train the Transformer to predict the velocity field  $v_\theta(z_t, t, c)$  that transports Gaussian noise  $z_1 \sim \mathcal{N}(0, I)$  to clean latents  $z_0$ , conditioned on text  $c$ .

*Noise-free condition injection.* Standard flow matching assigns a single scalar timestep  $t$  to every token in a sequence, making it impossible to distinguish tokens that should remain clean (conditioning frames) from those requiring denoising (generation targets). We address this by assigning **each token its own timestep embedding**. During training, we randomly select a prefix of  $F$  frames and set their per-token timestep to  $t=0$  (noise-free), while the remaining tokens receive  $t>0$ ; alternatively,  $F=0$  with probability 0.5 to train the text-to-motion mode. The timestep of each token is embedded via sinusoidal projection and MLP, and modulates the adaptive layer norm in each DiT block. This unified training procedure lets the model seamlessly learn both text-to-motion generation (all tokens noised) and pose-conditioned generation (prefix tokens clean) without any architectural change.

At inference, pose-conditioned generation is achieved by simply feeding the VAE-encoded conditioning frames as *noise-free tokens* with timestep 0 into the latent grid. The Transformer treats these clean tokens as context through self-attention while denoising the remaining tokens. This strategy requires no inpainting network, post-hoc blending, or task-specific modification. The key insight is that per-token timestep embeddings allow the model to *learn* the distinction between conditioning context and generation targets during training—a capability that is fundamentally unavailable when all tokens share a single scalar timestep.

*Autoregressive streaming.* Noise-free condition injection directly enables *autoregressive segment chaining*: the first segment is generated from text alone (pure text-to-motion); the last  $F$  frames are then VAE-encoded and injected as noise-free tokens into the next segment’s latent grid together with a new text prompt, and the process repeats. Each segment boundary is seamlessly shared without post-hoc blending, interpolation, or inpainting, because the generator has been trained to denoise around noise-free conditioning context.

*Self-forcing for drift suppression.* While noise-free chaining grants the model autoregressive streaming capability, prior autoregressive motion generation methods [1, 35] suffer from severe error accumulation over long rollouts: each segment’s condition comes from the model’s own previous output rather than ground truth, causing small errors to compound—manifesting as trajectory drift, motion degradation into static poses, and eventual collapse. This is fundamentally a *train–inference gap*: standard training uses *teacher forcing* where each segment is conditioned on ground-truth latents, but inference conditions on imperfect model outputs.

We adopt Self-Forcing [14] to close this gap. During training, the model generates a segment, decodes the output through the VAE, re-encodes it, and feeds the result back as the condition for the next segment—simulating the actual autoregressive inference pipeline. Distribution Matching Distillation [14] provides the training signal for these self-conditioned rollouts, teaching the model to remain stable when conditioned on its own imperfect outputs rather than clean ground truth. This enables stable generation over long rollouts with 10+ consecutive segments, far beyond the training horizon of  $\leq 360$  frames ( $\sim 12$ s at 30 fps).

*Narrative motion composition.* Prior long-horizon generation methods [1, 28, 35] require users to explicitly specify each atomic action and its duration. In practice, however, user inputs are often free-form narratives with implicit sub-actions and ambiguous timing (e.g., “A warrior approaches the gate, crouches behind the wall, then rolls to the side and stands up”). To bridge this gap, we employ a motion-aware text rewriter [33] that decomposes the narrative into a sequence of atomic action prompts, predicts the duration of each action, and rewrites the descriptions into a standardized form suitable for the generation model. PRISM then generates the full motion autoregressively via the segment-chaining mechanism described

above. In our evaluation (Sec 4.7), both PRISM and MotionStreamer [35] use the same decomposition and rewriting pipeline to ensure a fair comparison on generation quality alone.

## 4 Experiments

### 4.1 Setup

*Implementation.* The VAE uses three residual blocks with causal temporal convolutions (downsampling  $4\times$ ). Each frame is factorized into  $K=23$  tokens of dimension 6: one root token (3D position + 3D velocity), one global-orientation token, and 21 joint-rotation tokens (6D rotation [44]). Latent dimension  $D=16$ . Training: 400K steps, 16 V100 GPUs, batch 64/GPU, float32 only (bfloat16 causes collapse due to FK precision requirements), sequences  $\leq 360$  frames. The DiT follows Wan [31] and ViMoGen [16]: 30 blocks,  $\sim 1.4\text{B}$  parameters, T5-XXL [27] conditioning, 2D RoPE [29] along time and joint axes. Training: 300K steps, 80 V100 GPUs, batch 6/GPU, bfloat16. First-frame conditioning probability 0.5. Inference: 50 Euler steps, CFG scale 5.0.

*Training data.* We curate  $\sim 200\text{K}$  high-quality SMPL(-X) motion-text pairs from MotionHub [18], which aggregates and standardizes sequences from diverse open-source motion capture datasets with text annotations.

*Benchmarks and metrics.* We evaluate on four main settings plus a supplementary benchmark: (i) *Text-to-Motion*: on HumanML3D [10] and MotionHub, using R-Precision, FID, MM Dist, and Diversity computed with our trained TMR [25] features. (ii) *Pose-Conditioned Generation*: given a starting pose (1, 5, or 9 frames) and a text prompt, generate the corresponding motion; evaluated on both HumanML3D and MotionHub. (iii) *Long-Horizon Sequential Generation*: evaluated on BABEL [26] following FlowMDM [1], measuring subsequence quality and transition smoothness. (iv) *Narrative Motion Composition*: generating coherent multi-segment motion from free-form narrative text (50 scenarios, 10 categories); evaluated through a user study against MotionStreamer [35]. Additionally, we report MBench [16] results (9 physics-quality dimensions) in the appendix.

### 4.2 Text-to-Motion

Tab. 1 compares PRISM against both diffusion-based (ViMoGen [16], HY-Motion [33], MotionStreamer [35]) and discrete autoregressive methods (T2M-GPT [38], MoMask [9], Go-To-Zero [7]) on HumanML3D and MotionHub. All baselines operate on HumanML3D-native joint representations, whereas PRISM generates SMPL parameters and converts to joint positions via forward kinematics—a cross-representation setting that incurs evaluation overhead.

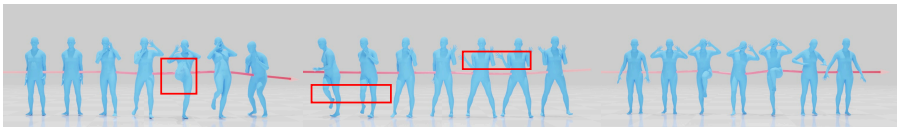
Despite this disadvantage, PRISM achieves state-of-the-art across all metrics on both benchmarks. On HumanML3D, FID drops 55% (0.027 vs. 0.060) and

**Table 1: Text-to-motion on HumanML3D and MotionHub.** All metrics are computed using our trained TMR features. “\*” denotes models retrained on the corresponding dataset. **Bold**: best; underline: second best.

Method	HumanML3D [10]					MotionHub				
	R-P T1↑	R-P T3↑	FID↓	MM-D↓	Div.→	R-P T1↑	R-P T3↑	FID↓	MM-D↓	Div.→
Real	0.778	0.906	0.000	0.901	21.69	0.667	0.842	0.000	0.984	22.96
ViMoGen [16]	0.152	0.299	0.405	1.203	19.71	0.157	0.308	0.532	1.213	20.02
MotionGPT3 [46]	0.410	0.631	0.375	1.115	20.88	0.200	0.369	0.449	1.184	21.04
MLD [4]	0.236	0.414	0.372	1.170	21.31	0.123	0.259	0.404	1.208	21.34
MoMask* [9]	0.249	0.429	0.369	1.157	20.91	0.160	0.346	0.432	1.194	21.60
MDM [30]	0.229	0.416	0.362	1.172	21.44	0.118	0.243	0.446	1.214	21.16
T2M-GPT [38]	0.362	0.585	0.337	1.127	21.48	0.146	0.285	0.460	1.212	21.02
MotionGPT [15]	0.310	0.504	0.326	1.151	21.29	0.127	0.248	0.439	1.238	21.16
HY-Motion [33]	<u>0.562</u>	<u>0.792</u>	0.186	1.062	22.39	<u>0.416</u>	<u>0.628</u>	0.363	1.145	<u>22.82</u>
Go-To-Zero [7]	0.443	0.653	0.078	1.051	<u>21.67</u>	0.293	0.461	<u>0.106</u>	<u>1.130</u>	<b>22.90</b>
MotionStreamer [35]	0.463	0.712	<u>0.060</u>	<u>1.029</u>	21.85	0.195	0.367	0.413	1.176	21.36
PRISM	<b>0.699</b>	<b>0.893</b>	<b>0.027</b>	<b>0.937</b>	<b>21.70</b>	<b>0.530</b>	<b>0.772</b>	<b>0.055</b>	<b>1.039</b>	22.76

R-Precision closes to within 1.4% of real motion (0.893 vs. 0.906). On MotionHub, FID improves 48% over Go-To-Zero (0.055 vs. 0.106). Diversity closely matches real data on both benchmarks, indicating no mode collapse.

A person **lifts one knee** while raising both hands **in front of the face** to maintain balance.



A person **steps forward** while throwing something with **the left hand**, then **steps back** to the original position.



GoToZero

ViMoGen

Ours

**Fig. 3: Qualitative comparison on text-to-motion.** PRISM produces smoother, physically plausible motions with less jitter and foot sliding than baselines.

### 4.3 Pose-Conditioned Generation

Noise-free condition injection enables pose-conditioned generation with zero architectural modification: the conditioning frames are VAE-encoded and injected as noise-free tokens (timestep 0) while the remaining tokens undergo standard denoising. We evaluate three conditioning granularities—1, 5, and 9 starting frames—on both HumanML3D and MotionHub, and compare against FlowMDM [1] and MotionStreamer [35].

**Table 2: Pose-conditioned generation on HumanML3D and MotionHub.** The model receives the first  $k$  frames as a noise-free condition together with a text prompt, and generates the remaining motion. All metrics are computed using our trained TMR features. **Bold**: best; underline: second best.

Method	Cond. Frames	HumanML3D [10]				MotionHub				
		R-P	T3 $\uparrow$	FID $\downarrow$	MM D $\downarrow$	Div. $\rightarrow$	R-P	T3 $\uparrow$	FID $\downarrow$	MM D $\downarrow$
Real motion	–	0.906	0.000	0.901	21.69	0.842	0.000	0.984	22.96	
FlowMDM [1]	1	0.430	0.358	1.176	21.38	0.288	<u>0.372</u>	1.179	21.18	
	5	0.441	0.347	1.168	21.46	0.298	<u>0.362</u>	1.172	21.27	
	9	0.453	0.338	1.162	<u>21.51</u>	0.312	<u>0.351</u>	1.167	21.34	
MotionStreamer [35]	1	<u>0.718</u>	<u>0.057</u>	<u>1.024</u>	<u>21.87</u>	<u>0.372</u>	0.408	<u>1.171</u>	<u>21.39</u>	
	5	<u>0.726</u>	<u>0.054</u>	<u>1.019</u>	<u>21.90</u>	<u>0.381</u>	0.396	<u>1.163</u>	<u>21.44</u>	
	9	<u>0.733</u>	<u>0.051</u>	<u>1.015</u>	21.93	<u>0.388</u>	0.387	<u>1.158</u>	<u>21.48</u>	
PRISM	1	<b>0.895</b>	<b>0.026</b>	<b>0.934</b>	<b>21.68</b>	<b>0.775</b>	<b>0.053</b>	<b>1.037</b>	<b>22.78</b>	
	5	<b>0.897</b>	<b>0.025</b>	<b>0.931</b>	<b>21.67</b>	<b>0.778</b>	<b>0.051</b>	<b>1.033</b>	<b>22.82</b>	
	9	<b>0.902</b>	<b>0.023</b>	<b>0.927</b>	<b>21.72</b>	<b>0.783</b>	<b>0.048</b>	<b>1.027</b>	<b>22.78</b>	

**Table 3: Sequential action generation on BABEL [26].** “Subseq.” evaluates per-segment motion quality; “Trans.” evaluates the smoothness at segment boundaries ( $\pm 15$  frames).

Method	Subseq. Quality				Transition Smoothness			
	R@3 $\uparrow$	FID $\downarrow$	Div. $\rightarrow$	MM D $\downarrow$	FID $\downarrow$	Div. $\rightarrow$	Peak Jerk $\rightarrow$	Area Jerk $\downarrow$
Real	0.638	–	21.24	0.978	–	19.83	0.010	0.000
DoubleTake [28]	0.400	0.140	21.08	1.152	0.110	19.50	0.040	0.850
FlowMDM [1]	0.460	<u>0.110</u>	<b>21.35</b>	1.094	<u>0.090</u>	<b>19.85</b>	<u>0.030</u>	<u>0.620</u>
MotionStreamer [35]	<u>0.469</u>	0.120	<u>21.38</u>	<u>1.073</u>	0.100	<u>19.70</u>	0.040	0.900
PRISM	<b>0.587</b>	<b>0.100</b>	21.43	<b>1.014</b>	<b>0.070</b>	20.57	<b>0.020</b>	<b>0.440</b>

As shown in Tab. 2, more conditioning frames improve both alignment and quality. PRISM handles pose conditioning natively via noise-free injection (conditioned frames at timestep 0), without the dedicated inpainting networks or blended encodings required by prior approaches [1, 28].

#### 4.4 Long-Horizon Sequential Generation

We evaluate long-horizon sequential generation on BABEL [26], where each test sample consists of a series of action segments described by individual text prompts. Following FlowMDM [1] and MotionStreamer [35], we set the transition length to 30 frames and report both *subsequence quality* (R@3 $\uparrow$ , FID $\downarrow$ , Diversity $\rightarrow$ , MM Dist $\downarrow$ ) and *transition smoothness* (FID $\downarrow$ , Diversity $\rightarrow$ , Peak Jerk $\downarrow$ , Area Under Jerk $\downarrow$ ).

As shown in Tab. 3, PRISM achieves state-of-the-art on both subsequence quality (R@3 0.587 vs. 0.469 for MotionStreamer) and transition smoothness

**Table 4: Motion tokenizer comparison on HumanML3D and MotionHub.** Reconstruction quality measured by rFID, MPJPE, PA-MPJPE, and MPJRE. All tokenizers are paired with the same 200M DiT for a fair comparison of latent space quality. **Bold**: best; underline: second best.

Method	HumanML3D [10]				MotionHub			
	rFID↓	MPJPE↓	PA-MPJPE↓	MPJRE↓	rFID↓	MPJPE↓	PA-MPJPE↓	MPJRE↓
MotionLCM [6] VAE	0.278	60.68	46.40	15.70	0.203	76.68	51.34	16.33
MotionStreamer [35] TAE	<u>0.020</u>	<u>33.82</u>	<u>26.11</u>	<u>7.75</u>	<u>0.355</u>	<u>59.83</u>	<u>45.64</u>	<u>14.42</u>
PRISM VAE (ours)	<b>0.001</b>	<b>1.82</b>	<b>1.10</b>	<b>0.35</b>	<b>0.001</b>	<b>1.99</b>	<b>1.24</b>	<b>0.28</b>

(Area Under Jerk 0.44, a 29% improvement over FlowMDM and 51% over MotionStreamer). Unlike DoubleTake’s inpainting or FlowMDM’s blended positional encodings, PRISM simply chains segments via noise-free condition injection with no post-hoc blending.

#### 4.5 VAE Reconstruction Comparison

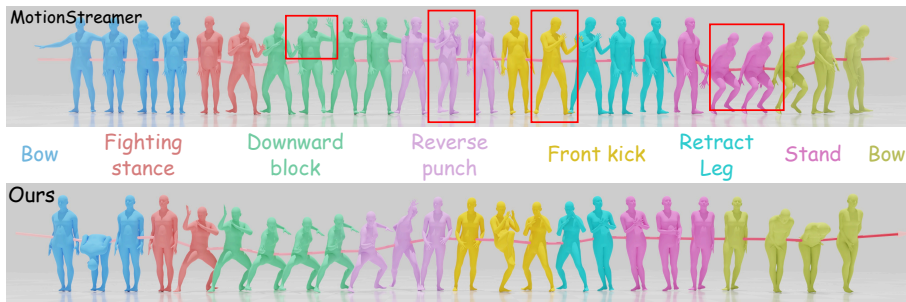


**Fig. 4: Qualitative comparison on long-horizon narrative composition.** PRISM follows all sub-actions with smooth transitions, while MotionStreamer misses several actions and exhibits drift.

To isolate the tokenizer’s contribution, we compare VAE architectures with a fixed 200M DiT (Tab. 4). Our joint-factorized VAE reduces MPJPE by  $18\times$  (1.82 vs. 33.82 mm) and rFID by  $20\times$  (0.001 vs. 0.020) on HumanML3D compared to MotionStreamer’s TAE, confirming that the structured 2D grid preserves motion detail far more faithfully than monolithic representations.

#### 4.6 Ablation Studies

We ablate the key design decisions of PRISM.

*Causal vs. non-causal convolution* (Tab. 5). The causal design is essential for seamless autoregressive chaining: it maintains competitive single-segment quality while enabling smooth multi-segment generation on BABEL.

**Table 5: Causal vs. non-causal Motion VAE.** Downstream generation quality on T2M (MotionHub), TP2M (HumanML3D, 1-frame), and BABEL sequential. Both variants share the same 1.4B DiT.

Temporal Conv.	T2M (MotionHub)				TP2M (HML3D)				BABEL Seq.		
	FID↓	R-P	T3↑	MM-D↓	FID↓	R-P	T3↑	MM-D↓	R@3↑	FID↓	MM-D↓
Non-causal	<b>0.051</b>	<b>0.779</b>	<b>1.034</b>	<b>0.029</b>	<b>0.891</b>	<b>0.941</b>	0.543	0.136	1.047		
Causal	0.055	0.772	1.039	0.031	0.887	0.946	<b>0.587</b>	<b>0.100</b>	<b>1.014</b>		

**Table 7: Autoregressive training strategy comparison on BABEL [26].** All variants share the same 1.4B DiT with noise-free condition injection.

Strategy	Subseq. Quality				Transition	
	R@3↑	FID↓	Div.→	MM D↓	Peak Jk.→	Area Jk.↓
No forcing (teacher)	0.574	0.118	<b>21.31</b>	1.028	0.05	0.91
Causal forcing	0.581	0.107	<b>21.38</b>	1.022	0.03	0.62
Self-forcing	<b>0.587</b>	<b>0.100</b>	21.43	<b>1.014</b>	<b>0.02</b>	<b>0.44</b>

*Joint-factorized (2D) vs. monolithic (1D) latent space (Tab. 6).* Factorizing the latent space into per-joint tokens dramatically improves both reconstruction (14× lower MPJPE) and generation quality (FID: 0.137→0.055).

**Table 6: 2D vs. 1D latent space.** Recon. and T2M gen. on MotionHub.

Latent	Recon.		T2M Gen.		
	rFID↓	MPJPE↓	FID↓	R-P T3↑	MM-D↓
1D (mono.)	0.018	28.47	0.137	0.614	1.103
2D (joint)	<b>0.001</b>	<b>1.99</b>	<b>0.055</b>	<b>0.772</b>	<b>1.039</b>

*Autoregressive strategies (Tab. 7).* We

compare three autoregressive strategies built on noise-free condition injection: (1) no forcing (teacher-forced training only), (2) causal forcing (conditioning on ground-truth previous segments at train time), and (3) self-forcing (conditioning on the model’s own generated latents during training to close the train–inference gap). Self-forcing suppresses drift in long-horizon rollouts by simulating the actual inference pipeline during training.

## 4.7 Narrative Motion Composition

Real-world applications often require generating motion from free-form narratives with multiple implicit actions. We term this task *narrative motion composition* and construct a benchmark of 50 diverse prompts spanning 10 categories, each describing 4–10 sub-actions (details in Appendix Sec. B). Both PRISM and MotionStreamer [35] use the same decomposition pipeline to isolate generation quality. In a GSB preference study with 20 evaluators (Tab. 8; protocol details in Appendix Sec. B), PRISM is judged “Good” (preferred) in >70% of trials across all four dimensions—motion quality, text fidelity, transition smoothness, and overall preference—with particularly strong margins on transition smoothness (78.1%) and overall preference (76.4%).

Fig. 3 and Fig. 4 show qualitative comparisons. On text-to-motion (Fig. 3), PRISM exhibits clear advantages in text-following fidelity and physical plausibility—characters perform described actions with accurate limb positioning and natural timing. On long-horizon narrative composition (Fig. 4), PRISM strictly follows all sub-actions with smooth segment transitions, while MotionStreamer misses several actions and exhibits trajectory drift over extended sequences. These qualitative results confirm the quantitative gains. Additional results and videos are on the project page.

## 5 Conclusion

We have presented PRISM, a streaming-capable motion generation framework built on two complementary ideas. A *joint-factorized motion latent space* assigns each body joint its own token, which a causal spatio-temporal VAE with FK supervision compresses into a structured 2D latent grid—the factorized space alone substantially surpasses monolithic latent approaches because the generator can model per-joint dynamics directly. *Noise-free condition injection* assigns each token its own timestep embedding, enabling a single flow-matching DiT to inject conditioning frames as clean tokens while denoising the rest, unifying text-to-motion, pose-conditioned generation, and unlimited-length streaming synthesis without task-specific modifications. With self-forcing, a model trained on clips of  $\leq 360$  frames ( $\sim 12$ s) stably generates long-horizon sequences with 10+ consecutive segments far beyond the training horizon. Extensive experiments on HumanML3D, MotionHub, BABEL, and a 50-scenario user study demonstrate state-of-the-art results—providing evidence that a structured latent space, rather than generator scaling alone, is key to the next quality leap in motion generation. Limitations and future directions are discussed in Appendix Sec. A.

## References

1. Barquero, G., Escalera, S., Palmero, C.: Seamless human motion composition with blended positional encodings. In: CVPR (2024)
2. Bian, Y., Zeng, A., Ju, X., Liu, X., Zhang, Z., Liu, W., Xu, Q.: Motioncraft: Crafting whole-body motion with plug-and-play multimodal controls. In: AAAI (2025)
3. Cai, Y., Wang, Y., Zhu, Y., et al.: A unified 3d human motion synthesis model via conditional variational auto-encoder. In: ICCV (2021)
4. Chen, X., Jiang, B., Liu, W., et al.: Executing your commands via motion diffusion in latent space. In: CVPR (2023)
5. Cho, J., Kim, J., Kim, J., Kim, M., Kang, M., Hong, S., Oh, T.H., Yu, Y.: Discord: Discrete tokens to continuous motion via rectified flow decoding. In: Proceedings of the IEEE/CVF International Conference on Computer Vision (ICCV). pp. 14602–14612 (October 2025)
6. Dai, W., Chen, L.H., Wang, J., Liu, J., Dai, B., Tang, Y.: MotionLCM: Real-time controllable motion generation via latent consistency model. In: ECCV (2024)
7. Fan, K., Lu, S., Dai, M., Yu, R., Xiao, L., Dou, Z., Dong, J., Ma, L., Wang, J.: Go to zero: Towards zero-shot motion generation with million-scale data. In: Proceedings

- of the IEEE/CVF International Conference on Computer Vision. pp. 13336–13348 (2025)
8. Gong, K., Lian, D., Chang, H., Guo, C., Jiang, Z., Zuo, X., Mi, M.B., Wang, X.: Tm2d: Bimodality driven 3d dance generation via music-text integration. In: Proceedings of the IEEE/CVF International Conference on Computer Vision. pp. 9942–9952 (2023)
  9. Guo, C., Mu, Y., Javed, M.G., et al.: Momask: Generative masked modeling of 3d human motions. In: CVPR (2024)
  10. Guo, C., Zou, S., Zuo, X., et al.: Generating diverse and natural 3d human motions from text. In: CVPR (2022)
  11. Guo, C., Zuo, X., Wang, S., Cheng, L.: Tm2t: Stochastic and tokenized modeling for the reciprocal generation of 3d human motions and texts. In: ECCV (2022)
  12. Han, B., Peng, H., Dong, M., et al.: Amd: Autoregressive motion diffusion. In: AAAI (2024)
  13. Hu, V.T., Yin, W., Ma, P., Chen, Y., Fernando, B., Asano, Y.M., Gavves, E., Mettes, P., Ommer, B., Snoek, C.G.: Motion flow matching for human motion synthesis and editing. arXiv preprint arXiv:2312.08895 (2023)
  14. Huang, X., Li, Z., He, G., Zhou, M., Shechtman, E.: Self forcing: Bridging the train-test gap in autoregressive video diffusion. In: NeurIPS (2025)
  15. Jiang, B., Chen, X., Liu, W., et al.: Motiongpt: Human motion as a foreign language. In: NeurIPS (2023)
  16. Lin, J., Wang, R., Lu, J., Huang, Z., Song, G., Zeng, A., Liu, X., Wei, C., Yin, W., Sun, Q., Cai, Z., Yang, L., Liu, Z.: The quest for generalizable motion generation: Data, model, and evaluation. In: ICLR (2026)
  17. Lin, J., Zeng, A., Lu, S., et al.: Motion-x: A large-scale 3d expressive whole-body human motion dataset. *Advances in Neural Information Processing Systems* **36**, 25268–25280 (2023)
  18. Ling, Z., Han, B., Li, S., Cheng, J., Shen, H., Zou, C.: Versatilemotion: A unified framework for motion synthesis and comprehension. arXiv preprint arXiv:2411.17335 (2024)
  19. Lipman, Y., Chen, R.T., Ben-Hamu, H., Nickel, M., Le, M.: Flow matching for generative modeling. In: ICLR (2023)
  20. Loper, M., Mahmood, N., Romero, J., Pons-Moll, G., Black, M.J.: Smpl: A skinned multi-person linear model. *ACM Transactions on Graphics* **34**(6) (2015)
  21. Lu, S., Wang, J., Lu, Z., et al.: Scamo: Exploring the scaling law in autoregressive motion generation model. In: CVPR (2025)
  22. Luo, M., Hou, R., Chang, H., et al.: An advanced multimodal, multitask framework for motion comprehension and generation. In: NeurIPS (2024)
  23. Peebles, W., Xie, S.: Scalable diffusion models with transformers. In: Proceedings of the IEEE/CVF international conference on computer vision. pp. 4195–4205 (2023)
  24. Petrovich, M., Black, M.J., Varol, G.: TEMOS: Generating diverse human motions from textual descriptions. In: ECCV (2022)
  25. Petrovich, M., Black, M.J., Varol, G.: Tmr: Text-to-motion retrieval using contrastive 3d human motion synthesis. In: ICCV (2023)
  26. Punnakkal, A.R., Chandrasekaran, A., Athanasiou, N., Quiros-Ramirez, A., Black, M.J.: BABEL: Bodies, action and behavior with english labels. In: CVPR (2021)
  27. Raffel, C., Shazeer, N., Roberts, A., et al.: Exploring the limits of transfer learning with a unified text-to-text transformer. *Journal of machine learning research* **21**(140), 1–67 (2020)
  28. Shafir, Y., Tevet, G., Kapon, R., Bermano, A.H.: Human motion diffusion as a generative prior. In: ICLR (2024)

29. Su, J., Lu, Y., Pan, S., Murtadha, A., Wen, B., Liu, Y.: RoFormer: Enhanced transformer with rotary position embedding. *Neurocomputing* **568**, 127063 (2024)
30. Tevet, G., Raab, S., Gordon, B., et al.: Human motion diffusion model. In: *ICLR* (2023)
31. Wang, A., Ai, B., Wen, B., Mao, C., Xie, C.W., Chen, D., Yu, F., Zhao, H., Yang, J., Zeng, J., et al.: Wan: Open and advanced large-scale video generative models. *arXiv preprint arXiv:2503.20314* (2025)
32. Wang, Y., Huang, D., Zhang, Y., et al.: Motiongpt-2: A general-purpose motion-language model for motion generation and understanding. *arXiv preprint arXiv:2410.21747* (2024)
33. Wen, Y., Shuai, Q., Kang, D., Li, J., Wen, C., Qian, Y., Jiao, N., Chen, C., Chen, W., Wang, Y., Guo, J., An, D., Liu, H., Tong, Y., Zhang, C., Guo, Q., Chen, J., Zhang, Q., Zhang, Y., Yao, Z., Zhang, C., Duan, H., Wu, X., Chen, Q., Cheng, F., Dong, L., He, P., Zhang, H., Lin, J., Zhang, C., Fan, Z., Li, Y., Hu, Z., Liu, Y., Jiang, J., Li, X., Bao, L.: HY-Motion 1.0: Scaling flow matching models for text-to-motion generation. *arXiv preprint arXiv:2512.23464* (2025)
34. Wu, Q., Zhao, Y., Wang, Y., Liu, X., Tai, Y.W., Tang, C.K.: Motion-agent: A conversational framework for human motion generation with llms. *arXiv preprint arXiv:2405.17013* (2024)
35. Xiao, L., Lu, S., Pi, H., Fan, K., Pan, L., Zhou, Y., Feng, Z., Zhou, X., Peng, S., Wang, J.: Motionstreamer: Streaming motion generation via diffusion-based autoregressive model in causal latent space. In: *ICCV* (2025)
36. Yang, H., Su, K., Zhang, Y., et al.: Unimuno: Unified text, music and motion generation. *arXiv preprint arXiv:2410.04534* (2024)
37. Yuan, W., Shen, W., He, Y., Dong, Y., Gu, X., Dong, Z., Bo, L., Huang, Q.: MoGenTS: Motion generation based on spatial-temporal joint modeling. In: *NeurIPS* (2024)
38. Zhang, J., Zhang, Y., Cun, X., et al.: Generating human motion from textual descriptions with discrete representations. In: *CVPR* (2023)
39. Zhang, J., et al.: The language of motion: Unifying verbal and non-verbal language of 3d human motion. In: *CVPR* (2025)
40. Zhang, M., Cai, Z., Pan, L., et al.: Motiondiffuse: Text-driven human motion generation with diffusion model. *IEEE Transactions on Pattern Analysis and Machine Intelligence* **46**(6), 4115–4128 (2024)
41. Zhang, M., Guo, X., Pan, L., Cai, Z., Hong, F., Li, H., Yang, L., Liu, Z.: Remodiffuse: Retrieval-augmented motion diffusion model. In: *ICCV* (2023)
42. Zhang, M., Jin, D., Gu, C., et al.: Large motion model for unified multi-modal motion generation. In: *ECCV* (2024)
43. Zhang, M., Li, H., Cai, Z., et al.: Finemogen: Fine-grained spatio-temporal motion generation and editing. In: *NeurIPS* (2023)
44. Zhou, Y., Barnes, C., Lu, J., Yang, J., Li, H.: On the continuity of rotation representations in neural networks. In: *CVPR* (2019)
45. Zhou, Z., Wang, B.: Ude: A unified driving engine for human motion generation. In: *Proceedings of the IEEE/CVF conference on computer vision and pattern recognition*. pp. 5632–5641 (2023)
46. Zhu, B., Jiang, B., Wang, S., Tang, S., Chen, T., Luo, L., Zheng, Y., Chen, X.: Motiongpt3: Human motion as a second modality. *arXiv preprint arXiv:2506.24086* (2025)

**Table 8: User study on narrative motion composition (GSB preference).** Percentage of trials where PRISM is judged Good / Same / Bad vs. MotionStreamer, by 20 evaluators on 50 narrative prompts (1,000 judgments per dimension). Both methods use the same decomposition pipeline.

Ours vs.	Motion Quality			Text Fidelity			Transition Smooth.			Overall Pref.		
	G↑	S	B↓	G↑	S	B↓	G↑	S	B↓	G↑	S	B↓
MotionStreamer	74.3	16.5	9.2	71.8	17.6	10.6	78.1	13.7	8.2	76.4	14.8	8.8

## A Limitations and Future Work

While PRISM achieves strong results on standard benchmarks, several directions remain for future work. First, our current model generates SMPL-22 body motion; extending to full SMPL-X with expressive hands and faces is a natural next step. Second, although our self-forcing strategy mitigates drift, very long sequences (>5 minutes) may still accumulate subtle trajectory errors, which could be addressed by incorporating global trajectory planning. Third, our model generates at  $\sim 20$  fps (SMPL-space), which, while practical for offline applications, is not yet sufficient for real-time interactive scenarios; distillation and architecture optimization may close this gap.

## B User Study Details

We provide the full protocol for the user study on narrative motion composition described in Sec 4.7.

*Task description.* Narrative motion composition takes a free-form narrative description as input—containing multiple implicit actions spanning 10–30+ seconds of motion—and generates a coherent, multi-segment 3D human motion sequence. Both our method (PRISM) and the baseline (MotionStreamer [35]) first decompose the narrative into atomic action prompts and rewrite each prompt with predicted duration using a motion-aware text normalization module [33], then generate motion autoregressively. This ensures the comparison isolates the generation quality from the planning and text normalization stages.

*Benchmark construction.* We construct a benchmark of 50 diverse narrative prompts spanning 10 categories (5 prompts per category):

- **Daily routine** — e.g., “A person wakes up from bed, stretches both arms overhead, yawns, walks to the bathroom, bends down to wash their face, then stands up and dries their face with a towel.”
- **Combat / martial arts** — e.g., “A martial artist takes a fighting stance, throws a left jab, follows with a right cross, ducks under a swing, delivers an uppercut, then steps back into guard position.”

- **Dance choreography** — e.g., “A dancer starts with arms at their sides, raises the right arm in an arc, spins on one foot, drops into a lunge, rises back up, sways hips left and right, then finishes with a dramatic pose.”
- **Sports / athletics** — e.g., “A gymnast runs forward, hurdles into a round-off, immediately does a back handspring, lands and takes a step, raises both arms in a salute, then walks back.”
- **Performance / theater** — e.g., “A mime pushes against an invisible wall on the left, then the right, then overhead, crouches down, discovers an invisible door handle, turns it, and steps through.”
- **Exercise / fitness** — e.g., “A person does five jumping jacks, drops for three push-ups, jumps to standing, performs two squat jumps, then rests with hands on knees.”
- **Social interaction** — e.g., “A person walks up, waves, joins a conversation circle, nods along, gestures broadly, laughs and leans back, looks at a watch, and waves goodbye.”
- **Occupational** — e.g., “A waiter carries an invisible tray, stops, carefully lowers it, sets items on the table, straightens up, tucks the tray under the arm, and walks away.”
- **Adventure / exploration** — e.g., “A hiker walks uphill, pulls themselves up a steep section, reaches the top, shields eyes to look into the distance, takes a deep breath with arms wide, then begins walking along the ridge.”
- **Narrative story** — e.g., “A person hears a noise, freezes, slowly turns to look behind, sees something alarming, takes two quick steps back, turns and sprints forward, then dives to the ground and covers their head.”

Each prompt describes 4–10 sub-actions. The benchmark is designed to stress-test autoregressive chaining, segment stitching, and the full decomposition pipeline.

*Evaluation procedure.* For each of the 50 prompts, both methods generate a motion video rendered from the same viewpoint with identical SMPL mesh visualization. Videos are presented to evaluators as anonymous, randomized pairs (labeled “A” and “B”). Evaluators do not know which method produced which result.

*Evaluation dimensions and protocol.* For each pair, evaluators make a **Good / Same / Bad (GSB)** judgment on four dimensions:

- **Motion Quality:** naturalness and physical plausibility of the generated motion (absence of jitter, foot sliding, ground penetration, and unnatural poses). “Good” = method A is clearly better; “Same” = no perceptible difference; “Bad” = method B is clearly better.
- **Text Fidelity:** semantic alignment between the narrative description and the generated motion (whether all described actions are correctly performed in the right order).
- **Transition Smoothness:** coherence at segment boundaries (whether transitions between consecutive actions appear natural and seamless, without abrupt jumps or freezing).

– **Overall Preference:** holistic quality judgment considering all of the above.

The GSB protocol reduces subjective noise compared to Likert-scale scoring: evaluators make a simple relative comparison rather than assigning absolute scores.

*Participants.* 20 evaluators participate in the study. All are graduate students or researchers with experience in computer vision or computer graphics. Each evaluator rates all 50 pairs, yielding 1,000 judgments per dimension (20 evaluators  $\times$  50 prompts). The study takes approximately 30–40 minutes per evaluator.

*Statistical analysis.* We report the percentage of trials judged Good (ours preferred), Same (tie), and Bad (baseline preferred) for each dimension. A binomial test is used to assess whether the Good rate significantly exceeds the Bad rate.

## C MBench Evaluation

We additionally evaluate on MBench [16], which probes nine dimensions of motion quality across three pillars: VLM-based (generalizability, condition consistency), physics-based (jitter, dynamics, foot floating, foot sliding, ground penetration), body penetration, and pose quality (Tab. 9). We note that the VLM-based metrics are still under development and may not fully reflect perceptual quality; we therefore present MBench results as supplementary evaluation rather than a primary comparison.

**Table 9: Results on MBench** [16]. MBench evaluates 9 dimensions across three pillars: *VLM-based* (generalizability, condition consistency), *physics-based* (jitter, dynamics, foot artifacts, ground penetration, body penetration), and *distribution-based* (pose quality).  $\uparrow$  = higher is better;  $\downarrow$  = lower is better. Scores are from the official MBench leaderboard except those marked with  $\dagger$  (evaluated by us).

Method	VLM		Physics				Body Pose		
	Gen. $\uparrow$	C.C. $\uparrow$	Jit. $\downarrow$	Dyn. $\uparrow$	F.Flt. $\downarrow$	F.Sld. $\downarrow$	G.Pen $\downarrow$	Pen. $\downarrow$	Q. $\downarrow$
Diffusion									
MDM [30]	0.51	0.42	0.014	0.038	0.156	0.014	0.134	1.68	2.67
MotionDiffuse [40]	0.42	0.44	0.011	0.029	0.126	0.006	0.076	1.35	2.21
FineMoGen [43]	0.42	0.37	0.012	0.039	0.281	0.009	0.141	1.18	2.28
MotionCraft [2]	0.45	0.42	0.013	0.042	0.402	0.009	0.137	1.15	2.12
MotionLCM [6]	0.55	0.48	0.022	0.044	0.193	0.020	0.151	1.73	2.40
ViMoGen-light [16]	0.55	0.47	0.013	0.029	0.155	0.005	0.059	1.43	2.10
ViMoGen [16]	0.68	0.53	0.011	0.025	0.204	0.006	0.076	1.78	2.38
HYMotion $\dagger$ [33]	–	–	0.008	0.037	0.087	0.004	0.000	1.71	2.46
Autoregressive / Masked									
T2M-GPT [38]	0.38	0.39	0.016	0.035	0.209	0.016	0.125	1.33	2.43
MoMask [9]	0.44	0.38	0.015	0.040	0.178	0.015	0.168	1.48	2.67
TM2T $\dagger$ [11]	–	–	0.024	0.039	0.293	0.022	0.080	1.31	2.57
TM2D $\dagger$ [8]	–	–	0.009	0.017	0.189	0.011	0.111	1.47	2.32
LoM $\dagger$ [39]	–	–	0.006	0.019	0.154	0.009	0.080	0.53	1.41
MotionGPT3 $\dagger$ [46]	–	–	0.012	0.040	0.157	0.020	0.095	2.24	3.18
Go-To-Zero $\dagger$ [7]	–	–	0.012	0.024	0.266	0.014	0.317	1.44	1.86
MotionStreamer $\dagger$ [35]	–	–	0.012	0.023	0.207	0.013	0.102	1.63	1.88
Ours (continuous latent)									
PRISM	–	–	0.009	0.036	0.183	0.017	0.089	1.56	2.48